

References not  
yet attached.  
DC7

# Solar Array Arcing in LEO

## How Much Charge is Discharged?

D.C. Ferguson\*, B.V. Vayner<sup>+</sup>, and J.T. Galofaro\*

NASA Glenn Research Center\* and Ohio Aerospace Institute<sup>+</sup>

**Abstract:** It is often said that only the solar array or spacecraft surfaces that can be reached by an arc plume are discharged in a solar array arc in LEO (Low Earth Orbit). We present definitive results from ground test experiments done in the National Plasma Interactions (N-PI) facility at the NASA Glenn Research Center that this idea is mistaken. All structure surfaces in contact with the surrounding plasma and connected to spacecraft ground are discharged, whether the arc plasma can reach them or not. Implications for the strength and damaging effects of arcs on LEO spacecraft are discussed, and mitigation techniques are proposed.

**Key Words:** solar arrays, low earth orbit, arcing, plasma interactions, arc plumes, mitigation

## 1. BACKGROUND

Modern solar arrays have areas of tens of square meters, and they operate with bus voltages exceeding 100 V. Electrostatic discharges (arcs) are undesirable and detrimental events for spacecraft function, and preventing these events and/or mitigating their consequences are of primary importance for spacecraft designers. Ground tests of small samples of large solar arrays have been used to provide the necessary information regarding arc inception voltages and expected arc damage for an entire array during its lifetime in space. However, the volume of the space plasma and the size of the test arrays that may be simulated in ground tests is limited by the size of the test vacuum chamber, and this fact necessitates the installation of additional capacitance between the sample and ground to simulate the actual capacitance of a spacecraft and its solar array discharging through the arc plasma. The magnitude of the capacitance to be added has been the subject of discussions for many years. If the discharge of a space solar array capacitance is caused by an arc plasma front propagating along the array surface, this magnitude is limited to about 1  $\mu\text{F}$ , because the array capacitance is approximately  $0.25 \mu\text{F}/\text{m}^2$ , and the propagation distance of the dense arc plasma is less than a few meters under the conditions of a typical LEO plasma.

On the other hand, if the entire array discharges through a current channel created by an arc, this capacitance can even reach  $10^3 \mu\text{F}$ . The amplitude and width of an arc current pulse are both increasing functions of the capacitance discharged, and that is why the damage inflicted on the solar array by an arc depends on the capacitance discharged in the arc. Is it the capacitance discharged by the dense arc-plasma front, or is it the much larger capacitance of the coverglasses of the entire array?

This is a preprint or reprint of a paper intended for presentation at a conference. Because changes may be made before formal publication, this is made available with the understanding that it will not be cited or reproduced without the permission of the author.

The experiments described below confirm that the entire array capacitance discharges through the arc current channel even under conditions when the arc-plasma front is prevented from propagating along the sample surface. Thus, the proper value for an additional capacitor must be high ( $\sim 10^3$   $\mu\text{F}$ ) for ground tests of arrays in order to properly simulate the damaging effects that may occur for arcs on spacecraft with large arrays.

## 2. EXPERIMENTAL SETUP

In our tests, the LEO space plasma was simulated in a large vacuum tank (2 m in diameter and 3 m high) equipped with four oil diffusion vacuum pumps that provided a background pressure about 0.5  $\mu\text{Torr}$ . One Kaufmann-type plasma source generated a xenon plasma with an electron temperature of 1-1.3 eV, an electron number density of  $(4-5) \times 10^5 \text{ cm}^{-3}$ , and a neutral gas pressure of about 50  $\mu\text{Torr}$ .

Two solar array samples (on fiberglass) were mounted on an aluminum sheet and installed vertically in the middle of the chamber (Fig.1). One sample (strings 1,2, and 3) represented a silicon solar array with UVR coverglasses of 300  $\mu\text{m}$  thickness. That corresponds to a capacitance of 4344 pF/string. Another sample (strings 4,5, and 6) had a capacitance of 7020 pF/string because of its thinner coverglasses (150  $\mu\text{m}$ ). The additional capacitor was chosen to have a capacitance of  $C = 0.03 \mu\text{F}$  ( $\pm 10\%$ ) for the convenience of measurements - such a choice provided comparable currents in all branches of the bias circuit. However, some measurements were done with a higher capacitance (0.25  $\mu\text{F}$ ) to reveal the dependence of the arc current pulse characteristics on the value of this capacitance. Four current probes provided measurements of discharge currents flowing in essential branches of the circuit (Fig.2). For the second series of measurements, a grounded aluminum plate was installed between the samples to prevent the propagation of the arc-plasma front from one sample to the other.

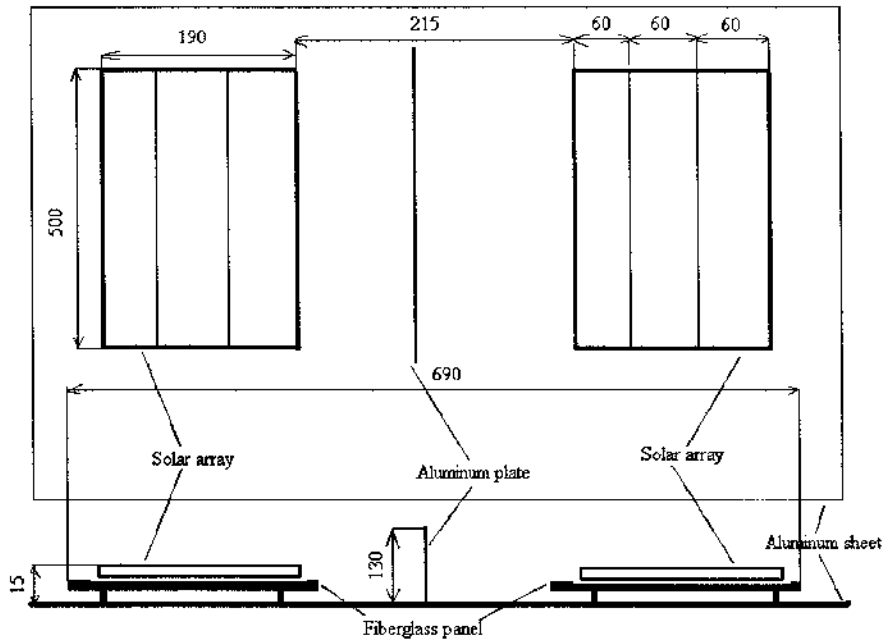


Figure 1. Two solar array samples are mounted on an aluminum sheet and installed vertically in a large vacuum chamber. All dimensions are shown in mm.

## 2.1 Experimental results

All four current pulse wave forms were registered by a four channel digital oscilloscope and stored in a computer for further processing. Twenty events (arcs) were observed for each configuration (positions of keys 1-4, and capacitance  $C$ ). That amounted to 260 files, one of which is shown in Fig.3. Each file was used to obtain the following data:

- 1)  $I_p$  - peak arc current; 2)  $\tau_{0.5}$  - pulse width at 0.5 of the peak current value; 3)  $\Delta q_i$  -net electrical charge flowed through the corresponding branch; 4)  $t_{ij}$  - time interval between current pulse peaks in the different circuit branches.

The magnitude of the net electrical charge flowing through a branch was calculated as

$$\Delta q_i = \int I_i(t) dt \quad (1)$$

Then, the average and standard deviation over several measurements were calculated, and the resultant value was compared with the theoretically predicted value. For example, the ratio of charges for string #1 ( $\Delta q_1$ ) and capacitor ( $\Delta q_2$ ) was calculated by

$$\frac{\Delta q_1}{\Delta q_2} = \frac{C_{string}}{C} \quad (2)$$

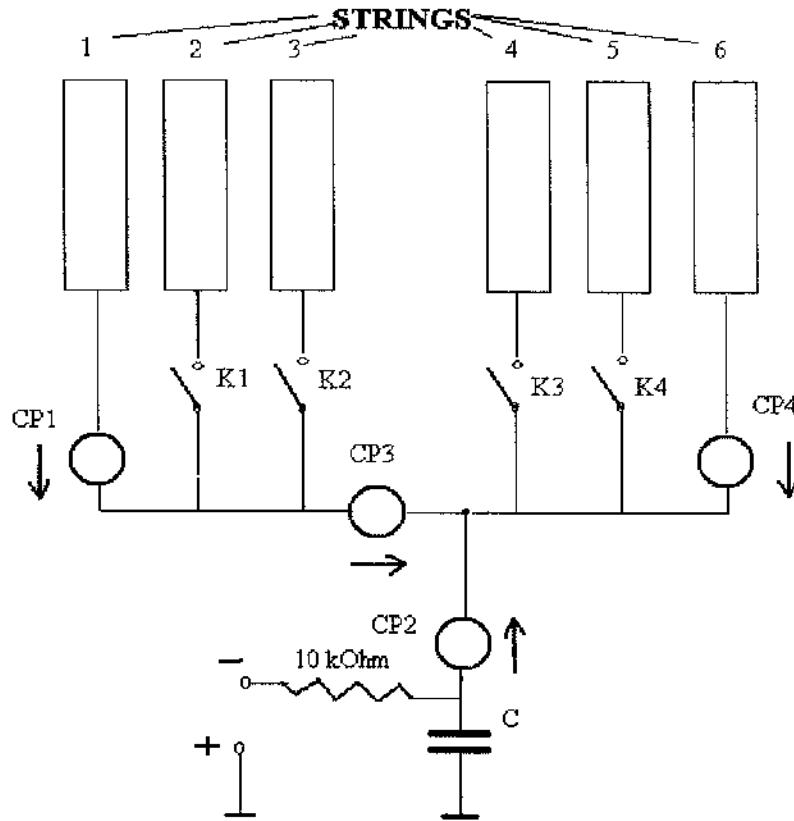


Figure 2. Four current probes were used to measure the discharge currents in four different branches of the circuit. The additional capacitance was chosen to be 0.03  $\mu\text{F}$  to obtain comparable current magnitudes for all probes. A few measurements were done with  $C=0.25 \mu\text{F}$ .

It should be noted that the possible errors in the calculations of string capacitances could not be estimated properly because of unknown errors in the corresponding geometrical and electrical parameters. However, the consistency of all or our final results is a very convincing argument that the calculations of array capacitances were done with an error of less than 10%. Also, the following ratio

$$\frac{\Delta q_{arc}}{\Delta q_2} = \frac{\sum C_{string} + C}{C} \quad (3)$$

was verified for all events when the experimental setup made it possible to do so. This equality means that the array capacitance that discharged through the arc current channel is independent of the distance between the arc site and other strings, and the array discharged fully with or without an aluminum plate installed between the two samples.

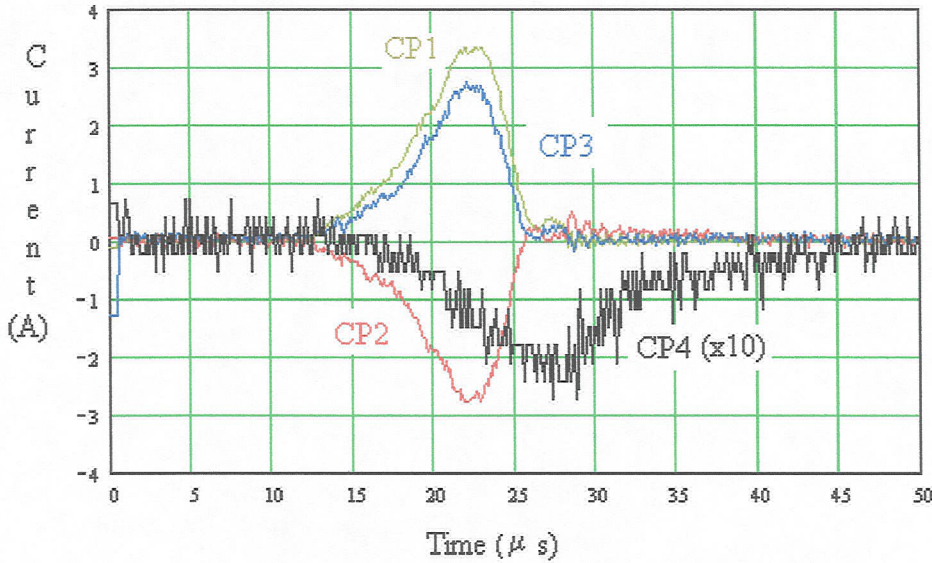


Figure 3. One example of an arc pulse current sequence for  $C=0.03 \mu\text{F}$ , and for switches K1&K2 in the closed position.

The results of our measurements and theoretical estimates are compiled in Table 1. Standard deviations ( $1\sigma$ ) of the measurements are shown in parenthesis.

Table 1.

No.	Key # :	Arc on :	$\frac{\Delta q_i}{\Delta q_2}$	$\frac{\Delta q_i}{\Delta q_2}$	$\frac{\Delta q_{arc}}{\Delta q_2}$	$\frac{\Delta q_{arc}}{\Delta q_2}$	Bias
	Closed :	string# :	measured :	estimate :	measured :	estimate	(V)
1	None	1	0.25(0.03)	0.234(0.02)	1.186(0.11)	1.379(0.05)	300
2	None	6	0.17(0.03)	0.145(0.015)	1.077(0.04)	1.379(0.05)	300
3	K	½	0.25(0.024)	0.234(0.02)	1.41(0.08)	1.52(0.06)	300
4	K1	6	0.16(0.02)	0.145(0.015)	1.22(0.08)	1.52(0.06)	300
5	K1&K2	2/3	0.25(0.026)	0.234(0.02)	1.4(0.08)	1.67(0.07)	300
6	K1&K2	6	0.217(0.06)	0.434(0.04)	1.49(0.07)	1.67(0.07)	300
7	K1&K2	2/3	0.26(0.034)	0.234(0.02)	1.43(0.1)	1.67(0.07)	280
8	K1&K2	6	0.21(0.05)	0.434(0.04)	1.46(0.1)	1.67(0.07)	280
9	All	4/5	0.19(0.05)	0.234(0.02)			280
10	All	2/3,6			1.85(0.06)	2.14(0.1)	280

The numbers shown in Table 1 demonstrate a very good agreement between the measured parameters and their theoretical estimates. We believe that some insignificant differences can be explained by our poor knowledge of the string capacitances, possibly by a somewhat incomplete discharge of the panels, and possibly by a somewhat inhomogeneous plasma potential distribution. However, the considerably smaller-than-expected discharge of strings 2&3 observed during two different runs cannot be explained to date. These results look particularly strange if one takes into account the very good agreement between the measurements for string#6 and its estimated values, because these two runs were supposed to be symmetrical to each other.

In the second stage of the experiment, an aluminum panel was installed between the two samples to prevent the propagation of the arc plasma from the arc site to the other sample (Fig. 1). Measurements were done with the same additional capacitor (0.03  $\mu\text{F}$ ,  $\pm 10\%$ ) and with another capacitor (0.22  $\mu\text{F}$ ,  $\pm 5\%$ ) connected in parallel with the first one. The results are shown in Table 2.

**Table 2.**

No.	Key #	Arc on	$\frac{\Delta q_i}{\Delta q_2}$	$\frac{\Delta q_i}{\Delta q_2}$	$\frac{\Delta q_{arc}}{\Delta q_2}$	$\frac{\Delta q_{arc}}{\Delta q_2}$	Bias	
		Closed	string#	measured	estimate	measured	estimate	(V)
1	K1&K2	2/3	0.21(0.03)	0.234(0.02)	1.32(0.07)	1.67(0.07)	450	
2	K1&K2	1	0.2(0.02)	0.234(0.02)	1.59(0.07)	1.67(0.07)	450	
3	K1&K2	2/3	0.03(0.004)	0.028(0.003)	0.956(0.02)	1.08(0.05)	400	
4	K1&K2	1	0.028(0.002)	0.028(0.003)	1.084(0.04)	1.08(0.05)	400	
5	K1&K2	2/3	0.191 (0.02)	0.234(0.02)	1.39(0.06)	1.67(0.07)	400	
6	K1&K2	1	0.203(0.024)	0.234(0.02)	1.63(0.1)	1.67(0.07)	400	

It can be seen from the data in Tables 1&2 that those strings which were not arcing discharged fully in both cases - with or without the aluminum panel between the samples. Thus, the mechanism of discharge of an entire array can only be explained by an electron current flowing from the negatively charge conductor (or semiconductor) to the surrounding plasma through the arc-plasma conductive channel. The positive charge of coverglass is neutralizing by ambient plasma electrons that are attracted by the positive potential of the coverglass.

The dependences of the arc current pulse width and amplitude on the net capacitance were found from the experiments shown in Table 1. However, the narrow range of capacitances used (0.042-0.064  $\mu\text{F}$ ) and large deviations in the measured values did not allow us to confirm (or to reject) any expected square root dependence (Fig 4).

For some measurements (shown in Table 2), a bigger additional capacitor (0.25  $\mu\text{F}$ ) was used, and this provided the opportunity to verify the expected dependence of the pulse width on the capacitance (Fig.5). It turned out that this dependence is slower than an expected (about 0.3 in power-law index, rather than the expected 0.5).

One more interesting feature of the discharge process is a time delay between the instant of the peaks in the arc-current pulse and in the discharge current of those strings not arcing (Fig.3). We believe that this delay is caused by a changing plasma potential during the discharge process (which corresponds to the spacecraft potential for LEO orbit). In actuality, in the simple situation when all keys (K1-K4) are open, and the arc occurs on string #1, the relaxation current on string #6 satisfies the following equation:

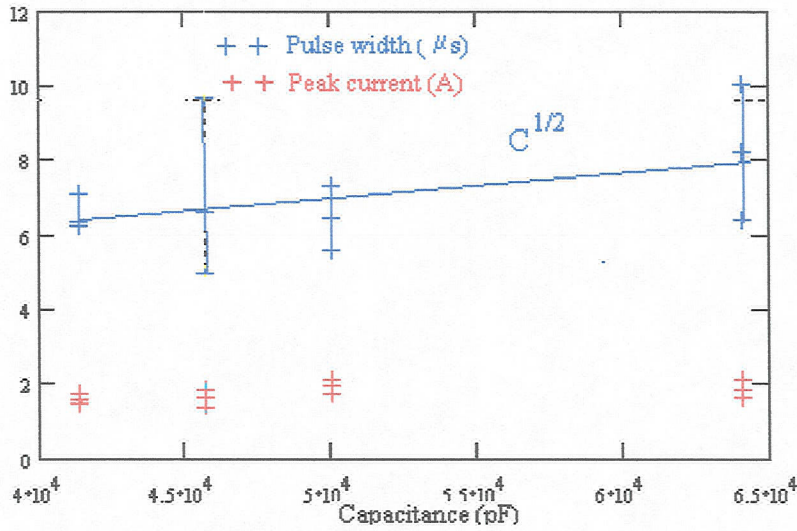


Figure 4. Arc current amplitudes and pulse widths vs. net capacitance are shown for the experiments without a conducting plate between the samples.

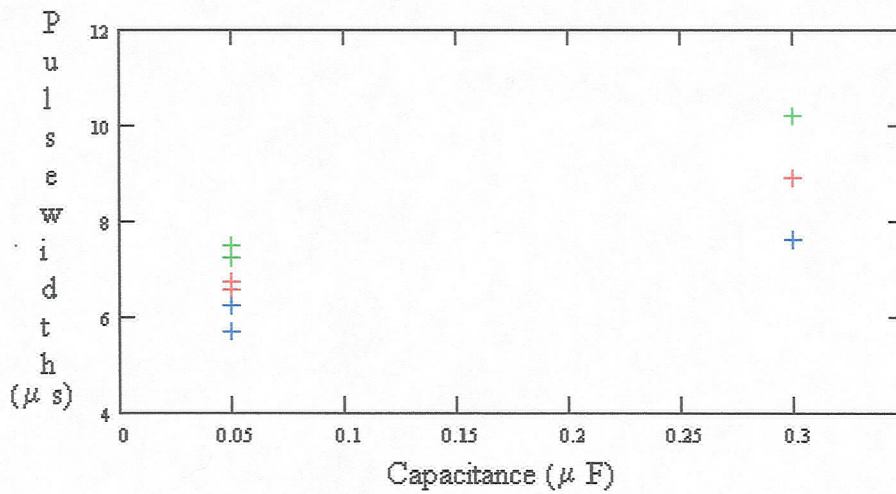


Figure 5. In spite of large deviations, a square root dependence of pulse width on capacitance can be excluded. The actual dependence is closer to a  $C^{1/3}$  dependence.

$$\frac{dI_4(x)}{dx} + I_4(x) = -\frac{C_{str}}{C} \cdot I_1(x) \quad (4)$$

where  $x = \frac{t}{\tau_{str}}$ , and  $\tau_{str}$  is the string relaxation time.

The solution of the Eq.4 with the initial condition  $I_4(0) = 0$  can be written as

$$I_4(x) = -\frac{C_{str}}{C} \cdot \exp(-x) \cdot \int_0^x I_1\left(\frac{C_{str}}{C}t\right) \cdot \exp(t) \cdot dt \quad (5)$$

If the arc current pulse is simulated by two exponents or by a Gaussian curve, the solution of Eq. (5) is shown in Fig.6.

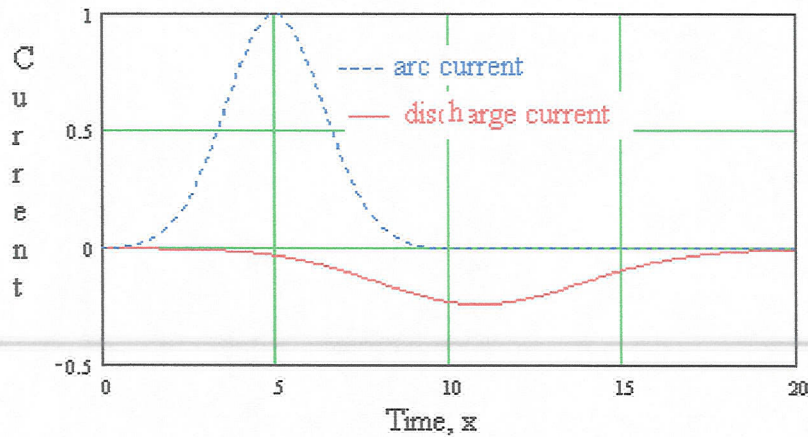


Figure6. The theoretical time delay between peaks of arc current and string discharge current is similar to the observed one.

### 3. CONCLUSION

The results of our current experiments and their analysis confirm the necessity of using a large additional capacitance (0.3-0.5 of the expected entire spacecraft solar array capacitance) in ground tests in order to adequately simulate the consequences of arcing on solar arrays in orbit.

### 4. APPENDIX

The measured time delay between current peaks in strings 1 and 6 was:

- 1) 280 V, no plate, 0.03 capacitor - 2.6(0.8)  $\mu$ s;
- 2) 450 V, plate, 0.03 capacitor - 4.88(1.68)  $\mu$ s.

### 5. REFERENCES